XXI IMEKO World Congress "Measurement in Research and Industry"
August 30 – September 4, 2015, Prague, Czech Republic

OPTIMAL OPERATION OF A THREE CAMERA SYSTEM ON A FOUR-WHEEL ROBOT

Jukka-Pekka Raunio, *Tuomas Välimäki, Risto Ritala*

Department of Automation Science and Engineering, Tampere University of Technology, Tampere, Finland,
jukka-pekka.raunio@tut.fi, tuomas.s.valimaki@tut.fi, risto.ritala@tut.fi

Abstract – At present the automated moving of a robot is made possible by a complete measurement system including GPS, laser scanners, radars and static cameras. Such approach is reliable but rather expensive. In this paper the optimal operation of a three camera system on a four-wheel robot is studied. The benefit of the dynamic camera system over the complete static measurement system is the reasonable price and the possibility to focus at certain directions.

Keywords: camera, robot, operation

1. INTRODUCTION

The first automated vehicle was introduced in 1980s [1]. Since then numerous research groups and companies have used a lot of effort to develop working automated vehicle prototypes. During the last few years the Google automated cars [2] and the Mercedes Benz robotic cars [3] have shown us that there exist increasingly interest and money around the automated moving vehicles. In [3], for example, the environment detection is based on four short-range radars, eight long-range radars, one stereo camera pair, and two single cameras. All cameras and radars are stationary pointing to the certain direction. Such system is obviously very expensive and requires a lot of algorithm development and sensor fusion increasing the price of the vehicles.

In animals the location of eyes differs whether you are a prey or a predator. Preys have eyes on the side maximizing the field of view [4],[5]. This helps them to rapidly detect any moving object which may be a threat. In predators the eyes are facing forward and the field of views are overlapping. This increases the certainty of the view which helps them to concentrate to their victim [4]. Overlapping of the views allows predators also to perceive depth information [4],[6]. In this paper the fact that the preys and the predator have the eyes in different location is used as a starting point in the optimal control of three cameras. In some cases the depth information of the target is relevant and thus the cameras are moved such that the field of the camera views are overlapping mimicking the eye location of the predators. Such approach enables the possibility to perceive 3D information with high accuracy [7]. However, in some cases the uncertainty of the surroundings of the robot is high which forces the robot to detect the environment with the maximum field of view mimicking the eye location of the preys.

Our research belongs to the research area of active sensing and sensor management. These areas are widely studied and recent publications related to this work are listed below. The camera system related work is studied in [8] and [9] in which the optimal orientation of camera in 3D reconstruction and the optimal arrangement of multi-camera system in surveillance applications are studied. In more general the active sensing in stochastic systems are studied for example in [10], [11],[12].

In this paper we are studying the optimal operation of a three camera system to gain the optimal information from the surrounding environment under some main task. In this work the main task is a target following task in the environment which consists of a moving object. Figure 1 visualizes the problem.

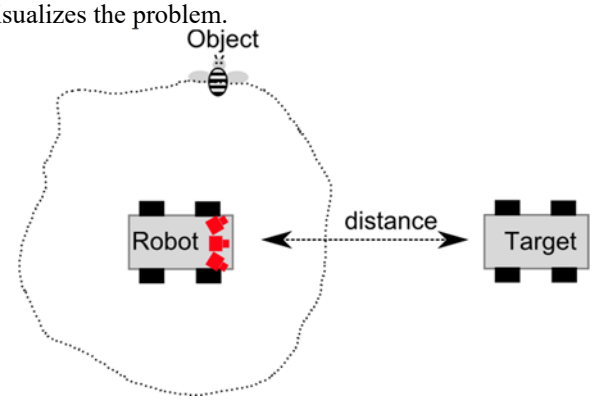

Fig. 1. Research problem: The goal is to control three cameras of robot such that the information from the distance of the target and the location of the object are maximized in the next time instant. Red boxes describe the cameras.

The depth information of the target is required to keep the distance between the robot and the target constant and prevent the collision. Also, the location of the moving object around the robot is relevant to know to prevent the collision with it. In more precisely, this paper introduces four measurement modes of cameras: 3D view mode to perceive the high accuracy depth information, 2D view mode to maximize the field of view, and 2D+3D views modes which combines the first two modes. The selection of the measurement mode is based on the entropy of the moving object and the distance accuracy of the followed target. The problem is solved for each time instant and it is assumed that each time instant is independent from the previous one in the camera mode sense; the problem to be solved is myopic.

This means that the camera mode can switch to any mode between the time instants. However, the probabilities related to the object entropy depend on the previous time instants making the problem dynamic. The entropy of the moving object increases in the areas invisible to the robot and decreases from the areas visible to the robot. Similarly depth accuracy of target increases when at least two cameras are facing to the target but decreases when the cameras field of views are not overlapping.

In this paper the developed method is tested in simulated environment. However, the paper introduces also robust moving object detection method from consecutive images and thus the developed method can be applied in the real-life cases.

This paper is organized as follows. In section 2 the robot and the camera-rig are introduced. In section 3 the moving object detection method and the camera control approach are presented. Section 4 shows the results. In last section the usability of the developed method in real-life applications is discussed and finally the work is concluded.

2. DESCRIPTION OF THE MEASUREMENT SYSTEM

The optimal control of a three camera system was designed to the ground robot with four wheels. The ground robot consists of the linux Ubuntu computer with robot operating system (ROS), the inertial motion unit, the odometry sensor and three machine vision cameras. All three measurements were connected to computer with usb cables; IMU and odometry with USB2 technology and machine vision cameras with USB3. All three machine vision cameras were manufactured by Point grey and the maximum resolution and the maximum imaging rate were, 4 Mpixels (2048 x 2048 pixels) and 45 Hz, respectively. The camera holders consist of two servos which can be tilted ±90° and panned ±90°. In this work the tilt of the cameras was fixed because the robot was applied indoors where the terrain can be assumed to be two dimensional. The field of view in each camera was 50°. Figure 2 shows the ground robot.

Fig. 2. The four-wheel robot. Three-camera rig can be seen on the top of the robot.

3. CONTROL OF CAMERAS

This paper introduces the method to operate a three camera system in a four-wheel robot. The operation problem is simplified by letting the cameras be only in four different modes. The modes are the 3D view mode to perceive the depth information with high accuracy, the 2D view mode to maximize the field of view, and the combined 2D and 3D view mode. The middle camera in our camera system is stationary and only the two outermost cameras can move. In the high accuracy 3D mode (Mode 1) all three cameras are turned to same direction thus the field of views are overlapping. In the Mode 2 and Mode 3 the field of view of two cameras overlap, and in the Mode 4 cameras are pointing to three independent directions. The possible modes are presented in Fig. 3.

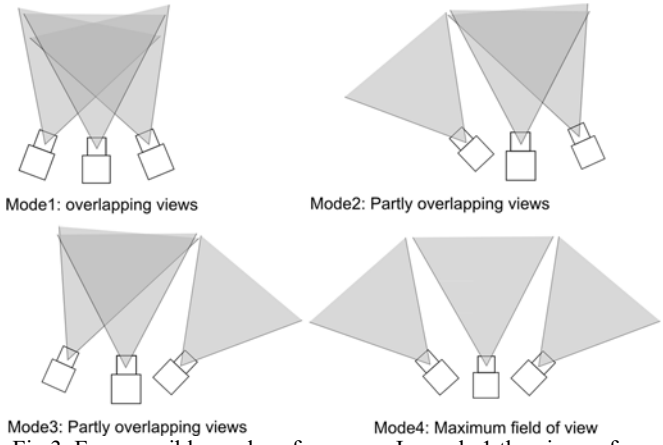

Fig 3. Four possible modes of cameras. In mode 1 the views of the all three cameras are overlapping increasing the certainty of depth computation. In mode 4 the field of view is maximized but the depth reconstruction is not possible. In mode 2 and 3 the views are partly overlapping providing depth information from the middle.

3.1. Detection of moving object from the image sequence

The selection of measurement mode is based on the entropy of the moving object and the distance of the followed target. The first research problem is to separate the moving object from the background. In this paper the target following task and the movement of object was simulated to minimize the possible error sources. The results are based on these simulated environments. However, the detection method of moving object from the image sequence is described in this chapter. Thus, the presented camera control method can be easily applied to real-life e.g the ground robot case.

The detection of the moving object is based on the optical flow templates and object detection from vector fields [13],[14]. In this paper introduced approach differs slightly from these articles. In this paper the optical flow vector fields are first median filtered in purpose to smooth the vector field. After that the vector fields are averaged over several time instances. Finally, the vectors which differ significantly from these averaged vectors are classified to moving objects. Such method removes the outliers and reveals the moving objects quite robustly when the speed of robot is constant. However, the fast change of course causes difficulties to separate the object from the fast moving background. This is a problem especially in small robots which speed is normally low and which can make sudden movements. Fig 4 shows an example of two image frames, smoothed vector field computed between the two frames, and the detected object (red rectangle).

The tracking problem will be also solved with optical flow approach. The template of followed target is determined and the optical flows vectors of the template are computed. The movement of the tracked object can be smoothed with Kalman filter for example.

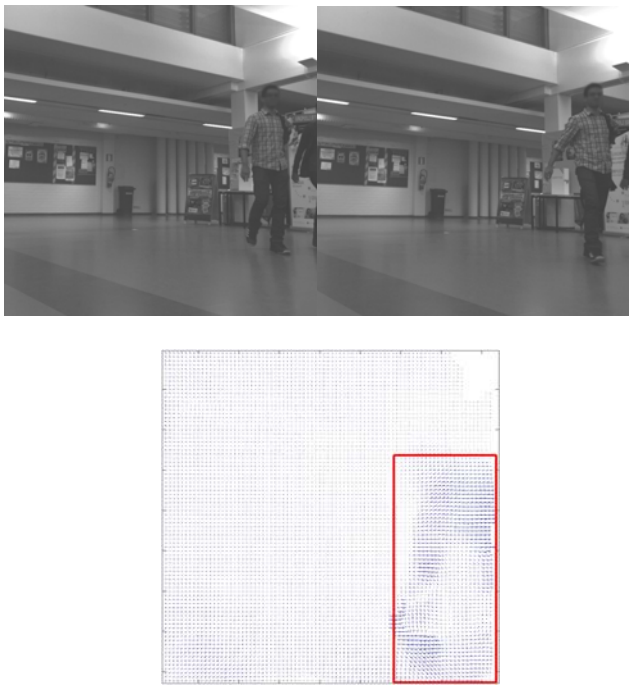

Fig 4. Two consecutive image frames (top) and the averaged and median filtered optical flow vector field between the frames (below). Red rectangle shows the detected moving object.

3.2. Probability of detection

The surroundings of the robot can be divided into the four different states which are shown in Fig.5. The state 0 locates behind the robot and therefore the detection from that state is not possible. The object can be detected from the state 1 only with the left camera and from the state 3 only with the right camera. All three cameras are able to see the object from the state 2.

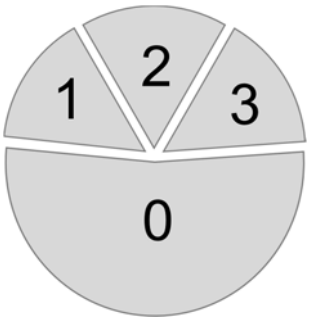

State	*opening angle*
0	210°
1	50°
2	50°
3	50°

Fig 5. The four possible states of the object. The left camera points to state 1 or 2 depending on the camera mode. The middle camera points always to state 2 and the right camera points to state 2 or 3 depending on the camera mode. Cameras are not able to see into the state 0. The opening angles of the states are based on the field of the view of cameras.

The camera can detect or cannot detect the object. The positive or negative detection is based on the state of the object, the camera mode and the uncertainty of detection. In this work the uncertainty of the detection is estimated with the probabilities. The probability of false positive detection (the object is detected even it not exists) is described with the $p_+^{(camera)}$ and the probability of false negative detection is described with $p_-^{(camera)}$ (the object is not detected even it exists) (*camera = 1,2,3*). Based on these uncertainty values the conditional probabilities of detection for each possible combination between the cameras, the states and the camera modes are computed. Table 1 shows an example of the probability table of the leftmost camera. The columns show the detection probabilities in four possible camera modes. The rows show how the state and the detection (*object detected = +, object not detected = -*) affects to the probability. The tables for the middle and the rightmost cameras are computed similarly (see appendix 1, table 3 and table 4).

Table 1. The detection probabilities of the leftmost camera. Table shows all combinations between the state, mode and the detection.

probability	mode 1	mode 2	mode 3	mode 4
$p(+\|state=0)$	$p_+^{(1)}$	$p_+^{(1)}$	$p_+^{(1)}$	$p_+^{(1)}$
$p(+\|state=1)$	$p_+^{(1)}$	$1-p_-^{(1)}$	$p_+^{(1)}$	$1-p_-^{(1)}$
$p(+\|state=2)$	$1-p_-^{(1)}$	$p_+^{(1)}$	$1-p_-^{(1)}$	$p_+^{(1)}$
$p(+\|state=3)$	$p_+^{(1)}$	$p_+^{(1)}$	$p_+^{(1)}$	$p_+^{(1)}$
$p(-\|state=0)$	$1-p_+^{(1)}$	$1-p_+^{(1)}$	$1-p_+^{(1)}$	$1-p_+^{(1)}$
$p(-\|state=1)$	$1-p_+^{(1)}$	$p_-^{(1)}$	$1-p_+^{(1)}$	$p_-^{(1)}$
$p(-\|state=2)$	$p_-^{(1)}$	$1-p_+^{(1)}$	$p_-^{(1)}$	$1-p_+^{(1)}$
$p(-\|state=3)$	$1-p_+^{(1)}$	$1-p_+^{(1)}$	$1-p_+^{(1)}$	$1-p_+^{(1)}$

The amount of possible detection permutation in three camera system is eight (see the table 2).

Table 2. All possible detection combinations between the cameras. Object detected = "+", object not detected = "-".

Leftmost camera (camera 1)	Middle camera (camera 2)	Rightmost camera (camera 3)
+	+	+
+	+	-
+	-	+
+	-	-
-	+	+
-	-	+
-	-	-

Next the probabilities of all detection combinations (=8) are computed in each possible state (=4) and each camera mode (=4) and the result is 8x4x4 tensor marked *p(detection|state,mode)*. The elements of the tensor are computed by using the probability matrices (see the table 1 and the table 2). For example, the probability to detect the object in state 2 with all three cameras(+++) in camera mode 1 can be computed as follows

$$p(+++|state = 2, mode = 1) = (1-p_-^{(1)})(1-p_-^{(2)})(1-p_-^{(3)}) \quad (1)$$

where $p_-^{(1)}$, $p_-^{(2)}$ and $p_-^{(3)}$ are the probabilities of false negative detection in leftmost, middle and rightmost cameras, respectively.

3.3. Camera mode selection

The selection of camera mode is based on the entropy of the object and the distance accuracy of the followed target.

In this paper the camera mode selection method is described based on the one moving object meaning that there exists one object in the surrounding areas of robot. The algorithm can be expanded into multi-object cases if necessary.

First the entropies of the object in four different states are computed. The entropies are calculated before and after the measurement and for each camera mode. The camera mode is selected such that it maximizes the entropy difference.

At the first iteration the probability of each state ($p(state)$) is estimated by dividing the opening angle of the state with the 360 degrees. The entropy [15] of the object in each possible state before the measurement can be determined based on the probabilities as follows

$$S_{state}^{before} = -p(state)\ln p(state) - (1-p(state))\ln(1-p(state)) \quad (1)$$

where the $p(state)$ $(state = 0,1,2,3)$ describes the probability of the object in the four possible states. Next the probability of the moving object after the measurement can be estimated for each camera mode and the detection by using the Bayes equation [10] as follows

$$p(state \mid detection, mode) = \frac{p(detection \mid state, mode)p(state)}{p(detection, mode)} \quad (2)$$

where the $p(detection,mode)$ is the overall probability of the detection determined as follows

$$p(detection, mode) = \sum_{\text{state}=0}^{3} p(detection \mid state, mode)\, p(state) \quad (3)$$

Next the *state* entropies ($S_{state,mode,detection}^{after}$) for each camera mode and for each detection are calculated by using the equation (1). The overall entropy in each *mode* is obtained by using the detection probabilities (3) as follows

$$S_{mode}^{after} = \sum_{state} \sum_{detection} S_{state,mode,detection}^{after}\, p(detection, mode) \quad (4)$$

These entropies are applied in the maximization problem which optimizes the camera mode in the next time instant.

Now we have determined the entropies to each possible camera modes for next time instant. Next, the distance accuracy of the target is determined based on the amount of cameras pointing towards the target. In the *mode 1* the accuracy is the highest, in the *mode 4* the accuracy is the lowest and in the *mode 2* and *mode 3* the accuracy is between the *modes 1* and *4*. Finally, the camera mode is selected such that the selection satisfies the following condition.

$$\max_{mode} \left[\lambda S_{mode}^{after} + (1-\lambda)sum(e)\right] \quad (5)$$

where λ is the weighting coefficient which determines the importance ratio between the object entropy and the distance accuracy of the target. The e is the goodness of the distance measurement accuracy in 3D point estimation.

The introduced method include constants such as distance accuracy of the camera modes, $p_{+}^{(camera)}$ and $p_{-}^{(camera)}$, which affect to the selection of camera mode. Therefore, the influence of constants to behaviour of selection is studied in the next chapter.

4. EXPERIMENTS AND RESULTS

This chapter presents the simulator applied in this work and describes experiments and results calculated in the simulated test environment.

4.1. Simulated test environment

Simulator was based on the random selection of *detection*. One of the possible *detection* options was selected based on the detection probabilities obtained in the equation (3). The dynamics of the simulator was achieved by updating the *state* probabilities of the object between the time instants. The updating equation was obtained from the state-space representation as follows

$$p(state)_{next} = \alpha_{state}(1-p(state)) + (1-\beta_{state})p(state) \quad (6)$$

where α_{state} and β_{state} describe probabilities that the object arrives into the *state* and that the object leaves from the *state*, respectively. The $p(state)_{next}$ is the state probabilities in the next time instant. The α_{state} values were selected such that their ratio between the *states* corresponds to the opening angle of the state obtained in Fig.4. Similarly the β_{state} values are selected such that their ratio between the states is inversely related to the opening angles.

The optimization was also based on the distance accuracy. It was assumed that the distance measurement is more important during certain time instants i.e. followed target is turning rapidly or the speed of the followed target is changing rapidly. In these conditions the high accuracy depth information is required which is provided by the camera *mode* 1. In normal conditions the distance between the robot and the target is rather stationary and the lower quality depth information is sufficient (*mode* 2, *mode 3*) or depth information is not required at all (*mode 4*). In this work the importance of distance measurement was simulated with random signal which was low pass filtered to achieve more realistic behaviour of the signal (see Fig. 6). The importance can vary between the range [0,1] where 1 means highest importance and 0 lowest importance.

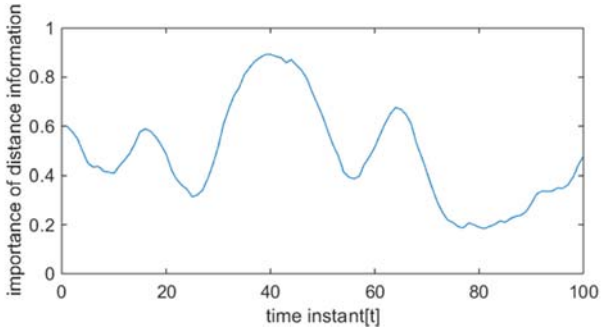

Fig. 6. The simulated importance of distance information.

4.2. Case 1: The accuracy in the distance measurements

This section studies the effect of the distance measurement accuracy to the distribution of selected modes. The depth accuracy of the multi-camera system depends on

the internal calibration of camera, the external calibration of the multiple cameras, the resolution of cameras, the lens quality and the number of cameras pointing to the target. In this work the calibration processes and the cameras are assumed to be similar and thus only the number of cameras affects to the distance uncertainty. First, the goodness of the distance measurement accuracy (range = [0, 1]) were set to 1 (*mode 1*), 3/4 (*mode 2 and 3*), and 0 (*mode 4*).The cameras are identical which means that the probabilities $p_{+}^{(camera)}$ and $p_{-}^{(camera)}$ are also equal. These values were set to 5%. The value λ was simulated as described in chapter 4.1. The simulator was executed 100 000 times and the distribution of selected *modes* and *detections* are presented in Fig. 7.

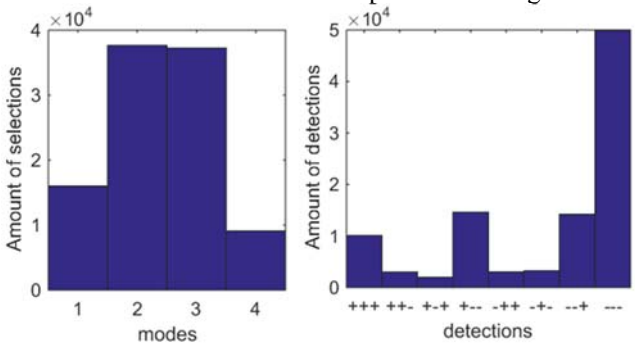

Fig. 7. The histogram of the selected modes (left) and the detections (right). The signs indicates the positive detection (+) and negative detection (-). The order of signs is: leftmost camera, middle camera and rightmost camera.

If the goodness of distance measurement accuracy ratio were set to 1 (*mode 1*), 1/2 (*mode 2 and 3*), and 0 (*mode 4*), the modes 1 and 4 became more popular. The results are shown in Fig.8 (left). Figure 8 (right) shows also the case when distance measurement accuracy in modes were 1 (*mode 1*), 9/10 (*mode 2 and 3*), and 0 (*mode 4*).

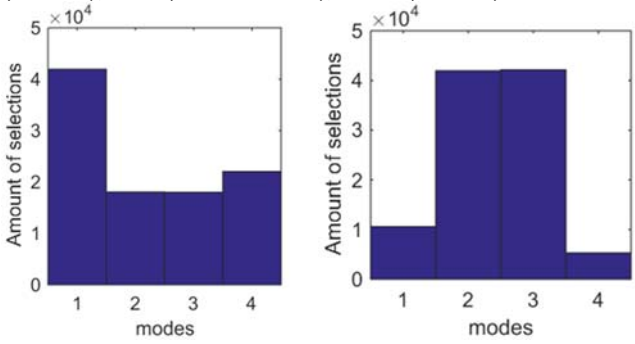

Fig. 8. The histograms of *modes* when the distance accuracy of *mode 2* and *3* are changed to 1/2 (left) and to 9/10 (right).

4.3. Case 2: The uncertainty in detection

In this section the effect of the detection uncertainty is studied. Detection uncertainty can be partly caused by the uncertainty in detection algorithm and partly by the fuzzy images. In this work both uncertainties are described with value-pair $p_{+}^{(camera)}$ and $p_{-}^{(camera)}$. In section 4.2 the detection uncertainty in each camera was 5 %. In this section the detection uncertainty is varied and the distance measurement accuracy was set to 1 (*mode 1*), 3/4 (*mode 2 and 3*), and 0 (*mode 4*). Figure 9 shows three examples in which the uncertainty of all cameras was set to 3%, to 15% and to 25%.

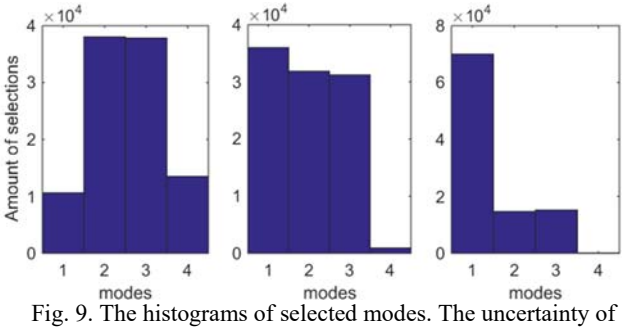

Fig. 9. The histograms of selected modes. The uncertainty of cameras was set to 3%, to 15% and to 25%.

It can be seen that when the uncertainty is high, the camera modes in which two or three cameras are pointed to same direction are preferred. The results also show that if the uncertainty to detect object is higher than 25%, the *mode 4* is never used in our measurement configuration.

5. DISCUSSION

This paper introduced the method to operate the three camera system based on the entropy of the moving object and the distance accuracy of the target. At the moment, the presented method is designed only for one moving object. However, the method can be easily generalized to several moving objects.

The developed method is planned to apply in the crowd or in the traffic in which the amount of moving object, relevant to the robot, is usually less than 10. The computation time of the developed method increases in a quadratic sense so the selection of optimal operation in the case of 10 moving objects is 1024 times slower than in one object case. However, in the Matlab® environment with the basic laptop we were able to optimize the camera *mode* 6000 times per second in the case of one moving object. Thus, the computation time is not a significant problem even with 10 moving objects if the computation is parallelized. However, the computation time starts to be a problem if the amount of moving objects is significantly more than ten or the amount of camera *modes* increases significantly. The one moving object method will be generalized to multi object case in the future work.

The presented method was developed to optimize the camera control of the three camera system. Furthermore, this paper presented an optimization tool which can be easily generalized to various situations. Such situations can be for example a system which includes several measurements (laser, camera, radar) and each measurement includes several measurement modes. Also, the introduced method is a powerful tool when the measurement systems are designed. The method reveals reliable if some measurement or measurement mode is useless (see Fig. 9 right) and thus the cost savings can be done already in the designing phase.

Our present approach assumes that the camera can switch between the *modes* arbitrary. However, this is not a realistic in real-life case when the robot operates over a long period of time. It is possible that the mode fluctuates between the mode 1 and 2 continuously which wear the servos quickly. In future studies the more advanced operation of cameras is introduced which takes into account several time instants ahead which will decrease the amount of possible fluctuation.

6. CONCLUSIONS

At the moment the automated moving is made possible by using GPS, laser scanner, radars and static cameras. Such approach is reliable but rather expensive. In this paper the optimal operation of a three camera system on a four-wheel robot was studied. The benefit of such system over the complete static measurement system is the reasonable price and the possibility to focus the measurement at certain directions around the robot. One interesting future research area is to compare performance of the developed method to the static camera-radar-laser -measurement system.

The camera operation method was based on the entropy of the moving object and the distance accuracy of the target. Such method takes into account all uncertainties in the measurement process which enables the applying the method in real-life applications. Furthermore, the method which detects moving objects from the image sequence was introduced. Thus, the developed method can be easily applied to real-life cases.

ACKNOWLEDGMENTS

The authors would like to acknowledge Juha Koljonen and Joonas Melin (TUT) for their contribution in the design and implementation of several electronic and mechanical parts of the measurement system. The authors express their gratitude to support by the academy of Finland project called "Optimal operation of observation systems in autonomous mobile machines" (O3-SAM).

REFERENCES

[1] C. Thorpe, M. Hebert, T. Kanade and S. Shafer, "Toward Autonomous Driving: The CMU Navlab. Part I: Perception", *IEEE Expert*, vol. 6, n°. 4, pp. 31 - 42, August, 1991.

[2] E. Guizzo, "How Google's Self-Driving Car Works", *IEEE Spectrum,* pp. 1-4, February, 2013.

[3] J. Dickmann, N. Appenrodt, C. Brenk, "Radar is the key to Mercedes-Benz's robotic car", *IEEE Spectrum*, pp. 41-45, August, 2014.

[4] E.T. Collins, *Arboreal life and the evolution of the human eye*, Lea and Febiger, New York, 1922.

[5] M. Cartmill, "New views on primate origins", *Evolutionary Anthropolgy: Issues, News and Reviews*, vol. 1, n°. 3, pp. 105 – 111, 1992.

[6] M. A. Changizi, "X-ray vision and the evolution of forward-facing eyes", *Journal of Theoretical Biology*, vol. 254, n°. 4, pp. 756 - 767, October, 2008.

[7] R. Hartley and A. Zisserman, *Multip View Geometry,* Cambridge University Press, Cambridge, UK, 2003.

[8] M. T. J. Spaan, P. U. Lima, "A decision-theoretic approach to dynamic sensor selection in camera networks", *In Int. Conf. on Automated Planning and Scheduling*, pp. 279–304, Thessaloniki, Greece, 2009.

[9] N. Atanasov, B. Sankaran, J. Ny, G. J. Pappas, K. Daniilidis, "Nonmyopic View Planning for Active Object Classification and Pose Estimation", *IEEE Transactions on Robotics*, vol. 30, n°. 5, pp. 1078–1090, 2014.

[10] R. Martinez-Cantin, N. De Freitas, E. Brochu, J. Castellanos, A. Doucet, "A Bayesian exploration-exploitation approach for optimal online sensing and planning with a visually guided mobile robot", *Autonomous Robots*, vol. 27, n°. 2 pp. 93–103, 2009.

[11] M. Lauri, R. Ritala, "Optimal Sensing via Multi-armed Bandit Relaxations in Mixed Observability Domains", *in Proc. IEEE Intl. Conf. on Robotics and Automation (ICRA)*, pp. 4807-4812, 2015, Seattle, WA, USA.

[12] B. Charrow, V. Kumar, N. Michael, "Approximate representations for multi-robot control policies that maximize mutual information", *Autonomous Robots*, vol. 37, n°. 4, pp. 383–400, 2014.

[13] R. Roberts and F. Dellaert, "Optical Flow Templates for Superpixel Labeling in Autonomous Robot Navigation".

[14] A. Giachetti, M. Campani, and V. Torre. "The use of optical flow for road navigation", *IEEE Transactions on Robotics and Automation*, vol. 14 n°. 1, pp. 34–48, 1998.

[15] C. M. Bishop, *Pattern Recognition and Machine Learning*, Springer, New York, USA, 2006.

APPENDIX 1

Table 3. The detection probabilities of the middle camera. Table shows all combinations between the state, mode and the detection.

probability	mode 1	mode 2	mode 3	mode 4
$p(+\|state=0)$	$p_+^{(2)}$	$p_+^{(2)}$	$p_+^{(2)}$	$p_+^{(2)}$
$p(+\|state=1)$	$p_+^{(2)}$	$p_+^{(2)}$	$p_+^{(2)}$	$p_+^{(2)}$
$p(+\|state=2)$	$1-p_-^{(2)}$	$1-p_-^{(2)}$	$1-p_-^{(2)}$	$1-p_-^{(2)}$
$p(+\|state=3)$	$p_+^{(2)}$	$p_+^{(2)}$	$p_+^{(2)}$	$p_+^{(2)}$
$p(-\|state=0)$	$1-p_+^{(2)}$	$1-p_+^{(2)}$	$1-p_+^{(2)}$	$1-p_+^{(2)}$
$p(-\|state=1)$	$1-p_+^{(2)}$	$1-p_+^{(2)}$	$1-p_+^{(2)}$	$1-p_+^{(2)}$
$p(-\|state=2)$	$p_-^{(2)}$	$p_-^{(2)}$	$p_-^{(2)}$	$p_-^{(2)}$
$p(-\|state=3)$	$1-p_+^{(2)}$	$1-p_+^{(2)}$	$1-p_+^{(2)}$	$1-p_+^{(2)}$

Table 4. The detection probabilities of the rightmost camera. Table shows all combinations between the state, mode and the detection.

probability	mode 1	mode 2	mode 3	mode 4
$p(+\|state=0)$	$p_+^{(3)}$	$p_+^{(3)}$	$p_+^{(3)}$	$p_+^{(3)}$
$p(+\|state=1)$	$p_+^{(3)}$	$p_+^{(3)}$	$p_+^{(3)}$	$p_+^{(3)}$
$p(+\|state=2)$	$1-p_-^{(3)}$	$1-p_-^{(3)}$	$p_+^{(3)}$	$p_+^{(3)}$
$p(+\|state=3)$	$p_+^{(3)}$	$p_+^{(3)}$	$1-p_-^{(3)}$	$1-p_-^{(3)}$
$p(-\|state=0)$	$1-p_+^{(3)}$	$1-p_+^{(3)}$	$1-p_+^{(3)}$	$1-p_+^{(3)}$
$p(-\|state=1)$	$1-p_+^{(3)}$	$1-p_+^{(3)}$	$1-p_+^{(3)}$	$1-p_+^{(3)}$
$p(-\|state=2)$	$p_-^{(3)}$	$p_-^{(3)}$	$1-p_+^{(3)}$	$1-p_+^{(3)}$
$p(-\|state=3)$	$1-p_+^{(3)}$	$1-p_+^{(3)}$	$p_-^{(3)}$	$p_-^{(3)}$